Contributed paper

OPTO-ELECTRONICS REVIEW **14**(2), 129–134

Nanometer-scale displacement sensing using self-mixing interferometry with a correlation-based signal processing technique

J. HAST*, M. OKKONEN, H. HEIKKINEN, L. KREHUT, and R. MYLLYLÄ

Optoelectronics and Measurement Techniques Laboratory, Infotech Oulu, University of Oulu, 90014 Oulu, Finland

A self-mixing interferometer is proposed to measure nanometre-scale optical path length changes in the interferometer's external cavity. As light source, the developed technique uses a blue emitting GaN laser diode. An external reflector, a silicon mirror, driven by a piezo nanopositioner is used to produce an interference signal which is detected with the monitor photodiode of the laser diode. Changing the optical path length of the external cavity introduces a phase difference to the interference signal. This phase difference is detected using a signal processing algorithm based on Pearson's correlation coefficient and cubic spline interpolation techniques. The results show that the average deviation between the measured and actual displacements of the silicon mirror is 3.1 nm in the 0–110 nm displacement range. Moreover, the measured displacements follow linearly the actual displacement of the silicon mirror. Finally, the paper considers the effects produced by the temperature and current stability of the laser diode as well as dispersion effects in the external cavity of the interferometer. These reduce the sensor's measurement accuracy especially in long-term measurements.

Keywords: self-mixing interferometry, laser diode, external cavity, Pearson's correlation coefficient, cubic spline interpolation.

1. Introduction

Self-mixing interferometry, also known as optical feedback or injection interferometry, is a promising technique for a variety of measurement applications involving interferometry [1]. Using a laser diode (LD) with an external cavity as interferometer, the technique offers several advantages over traditional interferometric configurations, such as Michelson, Mach-Zehnder and Sagnac. For example, the setup is very simple, compact and part-count-saving. Moreover, it does not require an external photodetector, because the interference signal can be picked up by the monitor photodiode of the LD package. In optical path length measurements, the technique offers subnanometer sensitivity, limited by the quantum detection regime [2]. Finally, the use of laser light also allows remote measurements.

The first demonstrations of this technique used a gas laser to detect the movements of a remote target [3]. Later on, LDs based on AlGaAs and InGaAs semiconductors operating in the 630–1600 nm wavelength range have been the most common light sources in self-mixing interferometry. One recent development involves using a blue wavelength GaN LD as light source [4]. The blue wavelength is a highly interesting alternative for future measurement applications in biotechnology and nanotechnology, since blue light is more responsive to different biomaterials than longer wavelengths. Additionally, blue light can also propagate through smaller apertures without diffraction. Self-mixing interferometry is a useful technique for MEMS applications to collect information from surrounding media or to operate as an internal sensor for moving parts in micro machines. A good example of using self-mixing interferometry in optical micro systems is the miniaturized multidirectional optical motion sensor introduced by Liess *et al.* [5].

Earlier papers on self-mixing interferometry have reported an accuracy of 40 nm in displacement measurements [6,7]. However, a double structured external cavity enables accuracy better than 10 nm [8]. In this paper, a self-mixing interferometer (SMI) based on a GaN LD is applied to nanometre-scale displacement measurements in the external cavity of the SMI. An external reflector, driven by a piezo (PZT) nanomover, is used to generate an interference signal between the laser cavity and the external cavity. This signal is detected using a monitor photodiode located at the back of the LD package. By varying the length of the external cavity, a phase difference is introduced into the interference signal. This phase difference can be detected using Pearson's correlation coefficient and cubic spline interpolation techniques. Results obtained from displacement measurements of the silicon mirror in the 0–110 nm range show that, in this displacement range, the average deviation between the measured and actual displacement of the mirror is 3.1 nm. Moreover, the results also show good linearity. Finally, the paper discusses the effects produced by the

*e-mail: jukka.hast@ee.oulu.fi

temperature and current stabilization of the LD as well as dispersion effects in the external cavity, which degrade the performance of the sensor, particularly in long-term measurements.

2. Self-mixing interferometer

Figure 1 presents the schematic arrangement of the SMI, consisting of an LD package with the LD cavity enclosed by the laser mirrors M_1 and M_2, a monitor photodiode and an external reflector, M_{ext}. Light emitted by the LD is guided to the external reflector, which reflects it back to the laser cavity, where this reflected light interacts with the original laser light, producing an intensity modulation in the output of the laser light. Intensity modulation caused by a movable external reflector is similar to that produced by a conventional optical interferometer, such that the fringe shift corresponds to an optical displacement of $\lambda/2$ [3]. The interference signal is detected using a monitor photodiode located at the backside of the LD cavity.

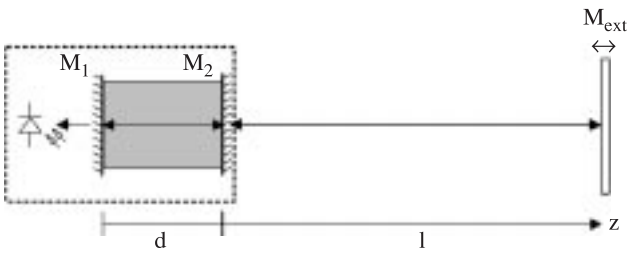

Fig. 1. Schematic arrangement of the SMI.

An analytical steady-state solution for the self-mixing signal can be written as [9]

$$P(\phi) = P_0[1 + mF(\phi)], \tag{1}$$

where P_0 it the power emitted by the unperturbed LD, m is the modulation index and $F(\phi)$ is the periodic function of the interferometric phase of the period 2π. The modulation index and $F(\phi)$ depend on the strength of the optical feedback, which differs from conventional two beam interferometry. The feedback parameter C is defined as [10]

$$C = \frac{\kappa s\sqrt{1+\alpha^2}}{dn_{las}}, \tag{2}$$

where α is the LD linewidth enhancement factor, s is the distance to the target, d is the length of the LD cavity and n_{las} is the cavity's refractive index. The coupling coefficient is defined as

$$\kappa = \frac{\varepsilon}{\sqrt{A}}\frac{1-R_2}{\sqrt{R_2}}, \tag{3}$$

where A represents total optical power attenuation in the external cavity, R_2 is the power reflection coefficient of the LD output mirror M_2 and ε is the factor accounting for the mismatch between the reflected and lasing modes. Different feedback levels are defined as a function of the parameter C as follows [1]. A very weak feedback regime occurs when $C < 1$ and the self-mixing signal is sinusoidal in shape. When C is in the range 0.1–1, SMI operates in the weak feedback regime, where the self-mixing signal gets slightly distorted and shows a non-symmetrical shape. In the moderate feedback regime, when C reaches values in the 1–4.6 range, the self-mixing signal becomes sawtooth-like and exhibits hysteresis. In the strong feedback regime, $C > 4.6$, the operation of the LD is no longer stable, leading to increased noise and mode hopping. In this case, the SMI is used in the weak feedback regime, where the shape of the interference signal is sinusoidal or slightly distorted.

Power fluctuations in the steady state operation of the LD in the weak feedback regime follow the equation [11]

$$\Delta P \approx g_c - g_{th} = -\frac{\kappa}{d}\cos(2\pi\nu\tau_{ext}), \tag{4}$$

where g_c is the compound threshold gain of the external and LD cavities, g_{th} is the threshold gain without feedback and ν is the optical frequency. τ_{ext} is the round-trip delay time in the external cavity defined as $\tau_{ext} = 2l/c$, where l is the length of the external cavity and c is the speed of light.

When the external target starts to move towards the LD with a constant velocity τ_{ext} changes as

$$\tau_{ext} = 2(l_0 - \nu_T t)/c, \tag{5}$$

where ν_T is the velocity of the target and t denotes the time. The ΔP function is now

$$\Delta P \approx g_c - g_{th} = -\frac{\kappa}{d}\cos(4\pi\nu_T t/c - 4\pi l_0\nu/c). \tag{6}$$

On the other hand, if the direction of the movement is towards the positive z-axis, the minus sign inside the brackets changes to a plus sign. When the fixed distance, l_0, changes to l_1, the phase term in Eq. (6) changes and can be detected as a phase shift in the self-mixing signal. This is illustrated experimentally in Fig. 3.

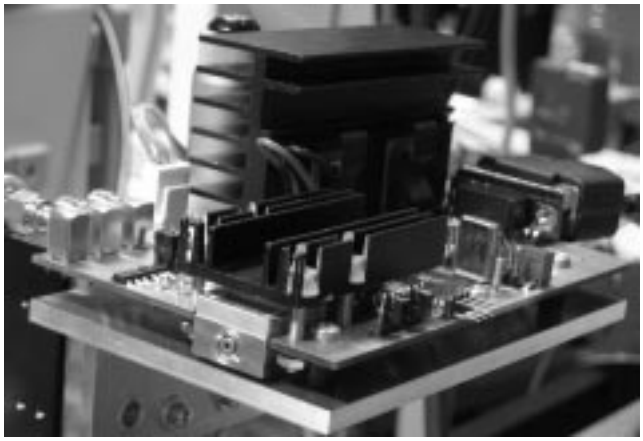

Fig. 2. Image of the SMI sensor head.

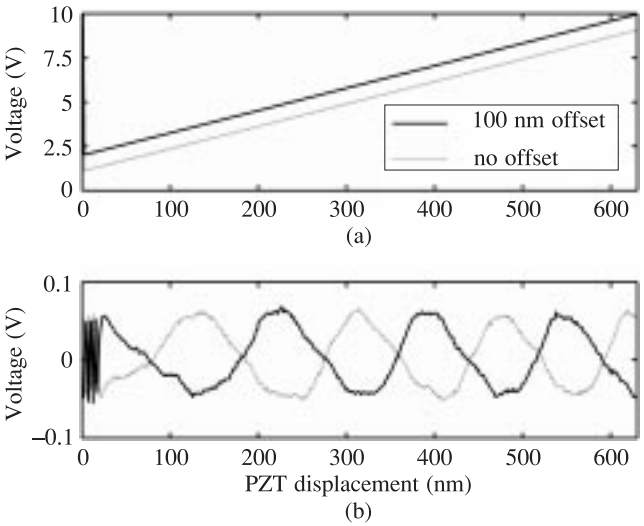

Fig. 3. Ramp signals which drive the PZT (a). Interference signals with and without a $\lambda/4$ offset (b). Ring-ring at the beginning of the interference signals is caused by the rapid return of the PZT back to start position.

3. Materials and methods

3.1. Measurement set-up

The SMI was constructed on a 12×8 cm aluminium board and consisted of a laser diode (LD) and its driver, amplifiers, a temperature controller and a digital computer interface. The laser was a commercially manufactured GaN LD, which emits blue light at 405 nm and has a threshold current of 47 mA at 21.0°C. To amplify the interference signal, the setup employed a DC-coupled preamplifier and an AC amplifier with a total transimpedance of 90 kΩ and a bandwidth of 13–40 kHz. A temperature controller stabilized the LD's operating temperature with a resolution of 0.1°C. Within the 1.5–10.6 mW power range, the sensor's optical power stability was better than 0.2%. The LD driver, the temperature controller and the sensor's data acquisition were all controlled by an ATMEGA128 on-board microcontroller, connected to a computer via an RS232 interface. In addition, the sensor had a wireless Bluetooth™ link, enabling remote control via a computer or a mobile device. For the purposes of this study, data acquisition was accomplished using an external 12-bit data acquisition card. Figure 2 shows an image of the SMI sensor.

Light emitted by the LD was first collimated and then focused on a mirror with a reflectivity of 96% at 405 nm, attached to a piezo (PZT) nanomover. The total length of the LD's external cavity was 11.5 cm, and the PZT was driven by a signal generator via a high power PZT driver. The signal generator, in turn, was monitored by a computer via a GPIB bus.

The computer started the measurement procedure by initiating both the SMI and the signal generator. The signal generator drove the PZT with a 10-Hz ramp signal whose amplitude was set to a voltage corresponding to a 630-nm displacement of the PZT. Next, the offset voltage of the PZT was changed such that it either pushed the mirror towards the LD or pulled it away from it. In other words, changing the offset voltage of the PZT allowed the fixed distance of the external cavity to be varied. As a result, the phase of the interference signal changed, as illustrated in Fig. 3, which presents the ramp and interference signals generated by the PZT with and without a $\lambda/4$ offset. The SMI signal is a periodic function showing a complete interferometric fringe each time the optical path length of the external reflector is varied by $\lambda/2$. In this case, when the length of the external cavity was changed by $\lambda/4$, ~100 nm, the interference signal with an offset was in the inverse phase relative to the signal without it.

3.2. Correlation-based signal processing technique

Several different methods have been used to detect phase information between two interference signals. For example, correlation studies involving self-mixing interferometry [12] have applied phase-locked [13] and fast Fourier transform techniques [14] to resolve phase information of the interference signal. In this study, a signal processing technique based on Pearson's correlation coefficient and cubic spline interpolation is utilized to determine the phase difference between two interference signals produced by changing the fixed distance of the external reflector in the external cavity of the LD. If one of the signals is a delayed version of the other, we may detect the delay by shifting one of signals and calculating the correlation coefficient for the overlapping parts of the two signals for every shift. As a result, we get a correlation of the signals as a function of lag, and the delay, or phase difference, between the original signals can be determined from the abscissa value of the correlation maximum. For the signals x and y of the length N, the equation for the correlation as a function of lag can be described as

$$c_{xy}(\tau_c)=\begin{cases}\dfrac{1}{N-\tau_c}\displaystyle\sum_{k=0}^{N-1}\dfrac{x(k)-\langle x\rangle^*}{\sigma_y^*}\dfrac{y(\tau+k)-\langle y\rangle^*}{\sigma_x^*}, \tau\geq 0\\ \dfrac{1}{N-\tau_c}\displaystyle\sum_{k=0}^{N-1}\dfrac{y(k)-\langle y\rangle^*}{\sigma_y^*}\dfrac{x(\tau+k)-\langle x\rangle^*}{\sigma_x^*}, \tau<0\end{cases}, \quad (7)$$

where $\langle x\rangle, \langle y\rangle, \sigma_x^*$ and σ_y^* are the mean and standard deviation of the overlapping parts of x and y. For Eq. (7), it is necessary to calculate the values only for $\tau_c < \tau_{max}$, where τ_{max} lies between the assumed maximum shift value and N-1. This eliminates unnecessary calculations, since only the maximum of $c_{xy}(\tau_c)$ is needed.

Interpolation is used to obtain values between the samples. This enables a better positioning of the correlation maximum, thereby improving the technique's phase detection resolution. The cubic spline interpolation technique used in this study involves fitting polynomial functions of

the third degree between the observed data values so that their first and second derivatives are the same at given values of $f(x_i)$, $i = 0\ldots n$. The polynomials are

$$p_i(x) = a_i x^3 + b_i x^2 + c_i x + d_i, x \in [x_{i-1}, x_i], i = 1\ldots n \quad (8)$$

and

$$p_i(x_{i-1}) = f(x_{i-1}), \qquad i = 1\ldots n$$

with the constraints

$$\begin{aligned} p_i(x_{i-1}) &= f(x_{i-1}), & i &= 1\ldots n \\ p_i(x_i) &= f(x_i), & i &= 1\ldots n \\ p_i'(x_i) &= p_{i+1}'(x_i), & i &= 1\ldots n \\ p_i''(x_i) &= p_{i+1}''(x_i), & i &= 1\ldots n-1 \\ p_i'(x_0) &= k_0 \\ p_n'(x_n) &= k_n. \end{aligned}$$

For each interval $[x_{i-1}, x_i]$, the coefficients a_i, b_i, c_i, and d_i are calculated and the maximum determined. Figure 4 presents the correlation coefficient as a function of phase for the signals shown in Fig. 3(b). Maximum correlation, 0.94, is obtained when the phase is 1.52 rad. At 405 nm, this corresponds to 98 nm, which is in good agreement with the measured signals.

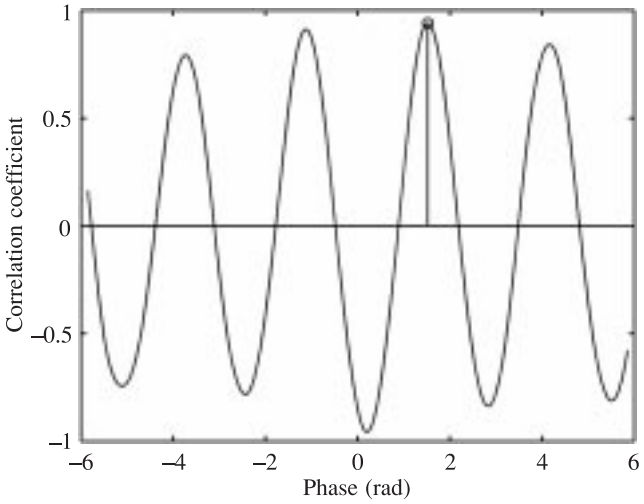

Fig. 4. Correlation of two interference signals.

4. Measurements and results

In the first experiment, the SMI was used to detect mirror displacements in the LD's external cavity. The offset voltage of the PZT was varied in the 0–15 V range with one volt steps. This voltage range corresponds to a 0–110 nm displacement of the external target. In terms of time, the offset voltage was altered at one second steps. All in all, the total measurement time was 15 seconds, during which time 10 measurements were conducted at each voltage step.

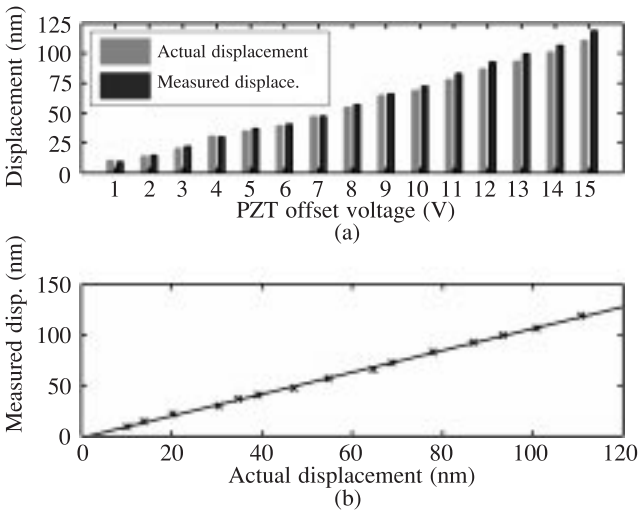

Fig. 5. Measured and actual displacements of the mirror as a function of the PZT offset voltage (a). Measured displacements as a function of the actual displacements and the linear fit (b).

After the measurements, the recorded analogue data were processed in the computer using the signal processing algorithm described earlier.

Figure 5(a) presents the measured average displacement using the SMI as a function of the PZT offset voltage. It also presents the actual displacement of the PZT, obtained from the PZT monitor output. In the 0–110 nm displacement range, the average deviation between the measured and actual displacement was 3.1 nm with a maximum deviation of 6.7 nm.

Figure 5(b) presents the measured displacement as a function of the actual displacement in the same offset voltage range. A linear fit using a linear mean square approximation is fitted to the data. The slope of the linear fit was 1.08, which is close to the unity and demonstrates that, within this range, the measurements follow the actual values linearly. The average deviation from the linear fit was 0.92 nm.

The next experiment illustrates what happens when the length of the external cavity is changed sinusoidally. In this experiment, the PZT offset voltage was varied in the 0–15–0 V range during a 10-s time period. Figure 6 presents the recorded interference signals. As the figure shows, when the offset voltage of the PZT was increased, the fringe pattern started to move left. Even in the opposite case, when the offset signal reached its maximum and started to decrease, the fringe patterns still moved to the left.

To better understand the behaviour of the SMI during long-term measurements, a set of experiments were carried out with measurement times exceeding a few minutes. It became apparent that in longer measurements the SMI system becomes vulnerable to several effects which reduce the sensor's performance. Among such effects are the LD's temperature and current stability as well as dispersion effects in the external cavity. Of these, temperature and cur-

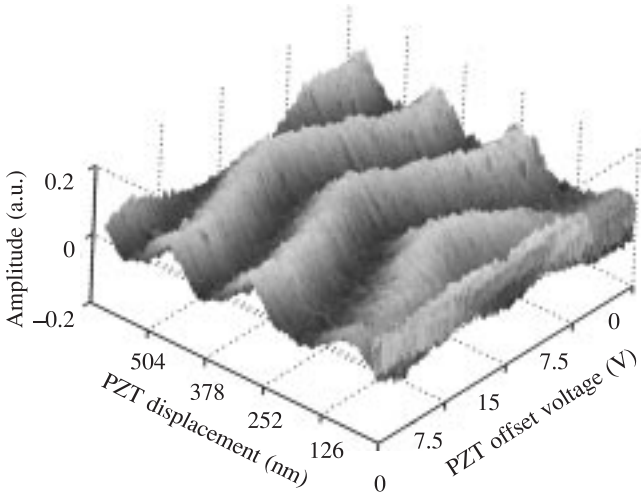

Fig. 6. Shift of the interference signal when the PZT offset voltage is changed sinusoidally.

rent stability are directly related to the lasing properties of the laser and have a clear effect on the SMI signal. In the free space setup, the SMI is sensitive to dispersion changes in the surrounding air caused by temperature variations in the measurement environment.

To demonstrate what effects these factors have on the stability of the interference signal, Fig. 7 displays the phase of the fringe maximum during a ten-minute measurement. During this measurement, only the ramp signal was applied to the PZT. As it can be seen, the phase of the fringe maximum drifts as a function of time. For the entire measurement, the standard deviation of this phase drift was 0.18 rad, corresponding to 11.7 nm at 405 nm. During measurement the period (a) the average change in the phase was less than 0.16 rad. On the other hand, during the period (b) the phase of the fringe maximum shifted approximately 0.78 rad, creating an error of $\lambda/8$. Thus, the success of measurements using this sensor depends strongly on this variation, particularly as the measurement time increases. However, for short-period measurements lasting less than a few tens of seconds, this effect is small. Consequently, it does not affect the detection of nanometre scale displacements in the external cavity of the SMI.

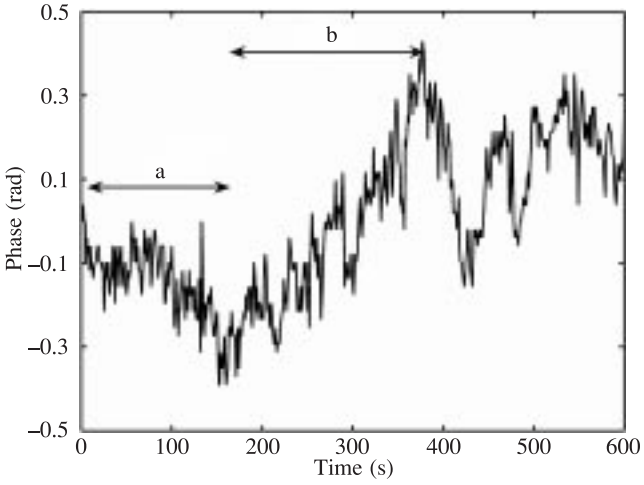

Fig. 7. Phase fluctuations of the fringe maximum during a 600-s-long measurement.

5. Discussion and conclusions

This paper studied nanometre-scale displacement sensing using self-mixing interferometry in a GaN laser diode. In addition, the paper described the operation of used the SMI sensor. Processing of the measured signals was performed using Pearson's correlation coefficient and the cubic spline interpolation technique. The target of the displacement measurements was a silicon mirror moved by a PZT nanomover, whose offset voltage was varied in the 0–15 V range in one volt steps. This voltage range corresponds to a 110-nm total displacement of the PZT. The average deviation between the measured and actual displacement was 3.1 nm. It was also found that the displacement measured using the SMI follow linearly the actual displacement of the PZT. In addition, the experiments demonstrated that the displacement of the target can be detected regardless whether the length of the external cavity increases or decreases.

This paper also showed that the phase of the measured interference signals drifts even in the absence of a stimulus. In our experiments, the average deviation of the phase of the fringe location was 0.18 rad. The greatest shift in the fringe location, $\lambda/8$, was obtained with a time constant of 250 s. Limits on the accuracy of the self-mixing interferometer are imposed by the fact that the LD's emission wavelength depends on its drive current and temperature. For example, Ref. 15 reports achieving an accuracy of approximately 0.4 μm in displacement measurements using a single-mode Fabry-Perot type laser diode with a temperature of 0.01°C and a current stabilization range of ±10 μA. Due to manufacturing reasons, the coefficients of the drive current and temperature stability of the used GaN laser diode were unknown to us. Nevertheless, the temperature stability of the GaN laser should be improved for better long-term stability.

Another factor with an adverse affect on the stability of the interference signal is the dispersion of air in the external cavity. To provide an estimate of the refractive index of air, we may utilize an updated Edlén equation [16]. Based on this equation, it has been calculated that a one-degree variation in temperature causes a one-ppm change in the refractive index at 15°C and 760 mbar [9]. For a 10-cm external cavity, a one-degree temperature variation changes the optical distance by 10 nm.

Self-mixing interferometry offers an interesting readout technique for different interferometric measurement applications in MEMS, biotechnology and nanotechnology. Moreover, blue light allows the measurement of smaller objects than longer wavelengths. Also, many biomaterials show an increase in activity as the wavelength decreases. One disadvantage of using GaN lasers is that they are still relative expensive. In addition, as monitor diodes, they use

standard silicon photodiodes, which have a rather low sensitivity, approximately 400 nm. As a result, GaN lasers require high gain electronics, which increases noise and may cause stability problems.

Acknowledgements

The authors would like to extend their warmest thanks to the Infotech Oulu Graduate School for financial support.

References

1. G. Giuliani, M. Norgia, S. Donati, and T. Bosch, "Laser diode self-mixing technique for sensing applications", *J. Opt. A: Pure Appl. Opt.* **4**, 283–294 (2002).
2. G. Giuliani, S. Bozzi-Pietra, and S. Donati, "Self-mixing laser diode vibrometer", *Meas. Sci. Technol.* **14**, 24–32 (2003).
3. M.J. Rudd, "A laser Doppler velocimeter employing the laser as a mixer-oscillator", *J. Phys. E: Sci. Instrum.* **1**, 723–726 (1968).
4. J. Hast, L. Krehut, and R. Myllylä, "A displacement sensor based on optical feedback interferometry in a GaN laser diode", *Opt. Eng.* **48**, 080504 (2005).
5. M. Liess, G. Weijers, C. Heinks, A. Horst, A. Rommers, R. Duijve, and G. Mimnagh, "A miniaturized multidirectional optical motion sensor and input device based on laser self-mixing", *Meas. Sci. Technol.* **13**, 2001–2006 (2002).
6. S. Merlo, and S. Donati, "Reconstruction of displacement waveforms with a single-channel laser diode feedback interferometer", *IEEE J. Quantum Electron.* **33**, 526–531 (1997).
7. F. Gouraux, N. Servagent, and T. Bosch, "A phase-modulated method to improve the resolution of a self-mixing interferometer", *Proc. IEEE-LEOS ODIMAP II*, 81–86 (1999).
8. M. Wang and G. Lai, "A self-mixing interferometer using an external dual cavity", *Meas. Sci. Technol.* **14**, 1025–1031 (2003).
9. S. Donati, *Electro-optical Instrumentation*; *Sensing and Measuring with Lasers*, Upper Saddle River, NJ; Prentice-Hall, 2004.
10. G.A. Acket, D. Lenstra, A.J. den Boef, and B.H. Verbeel, "The influence of feedback intensity on longitudinal mode properties and optical noise in index guided semiconductor lasers", *IEEE J. Quantum Electron.* **20**, 1163–1169 (1984).
11. M.H. Koelink, M. Slot, F.F.M. de Mul, J. Greve, R. Graaff, A.C.M. Dassel, and J.G. Aarnoudse, "Laser Doppler velocimeter based on the self-mixing effect in a fiber-coupled semiconductor laser: theory", *Appl. Opt.* **31**, 3401–3408 (1992).
12. S.K. Özdemir, S. Ito, S. Shinohara, H. Yoshida, and M. Sumi, "Correlation-based speckle velocimeter with self-mixing interference in a semiconductor laser diode", *Appl. Opt.* **38**, 6859–6865 (1999).
13. T. Suzuki, S. Hirabayashi, O. Sasaki, and T. Maruyama, "Self-mixing type of phase locked laser diode interferometer", *Opt. Eng.* **38**, 543–548 (1999).
14. M. Wang, "Fourier transform method for self-mixing interference signal analysis", *Opt. Laser Technol.* **33**, 409–416 (2001).
15. S. Donati, G. Giuliani, and S. Merlo, "Laser diode feedback interferometer for the measurements of displacements without ambiguity", *IEEE J. Quant. Electron.* **QE-31**, 113–119 (1995).
16. K.P. Birch, and M.J. Downs, "An updated Edlén equation for the refractive index of air", *Metrologia* **30**, 155–162 (1993).

